In Vitro Photo-Catalytic Degradation of Chloramphenicol Using Pharmaceutical Wastewater

G. Mahendran and G. Arthanareeswaran*

Membrane Research Laboratory, Department of Chemical Engineering, National Institute of Technology, Tiruchirappalli–620 015,Tamil Nadu, India

Abstract: In this work, the performance of composite membranes for the treatment of Chloramphenicol (CAP) pollutants was investigated from pharmaceutical industrial wastewater. The composite membrane was under operated with different concentrations of CAP with Titanium dioxide (TiO_2) in 10mg/L, 20mg/L and 30 mg/L. The composite membranes were cross-linked with glutaraldehyde for the elimination of H_2SO_4. Characterizations of synthesized composite membranes were carried out to analyze functionality, morphology, and hydrophilic behaviours. In continuous operation, the different time intervals of TiO_2 were removed in centrifuging. The performance of the composite membrane is the removal of pollutant CAP by UV analysis, and kinetics model at different concentrations. The degree of swelling and contact angle were measured in different concentrations of CAP at TiO_2. Liquid Chromatography (LC) is used to CAP with Titanium dioxide mixtures. Mass Spectrometry (MS) can be used for structural identity with high specificity. The MS is also used to analyze CAP from pharmaceutical industrial wastewater. The membranes were subjected to filtration of pharmaceutical wastewater which gave a maximum rejection of 95% of Chloramphenicol.

Keywords: Pharmaceutical wastewater, Cellulose acetate (CA), Cellulose triacetate (CTA) composite membrane, Titanium dioxide (TiO_2), Chloramphenicol (CAP).

1. INTRODUCTION

Global population growth and medical developments have resulted in a considerable and growing demand for pharmaceuticals during the last few decades. In developing nations such as India, medications are over prescribed. Despite the fact that diverse pharmaceutical drugs have significant benefits, including saving and prolonging lives, casing suffering and improving the overall quality of life, vast amounts of pharmaceutical-contaminated effluent have been released into the environment. The contamination of both surface water and land water as a result of the existence of these medications is a major issue in the twenty-first century. Antibiotics are a class of drugs with low biodegradability and high toxicity [1, 2]. A trace amount of toxics pharma compounds in drinking water may cause serious effects to human and animal like health and life. However, the concentrations of toxics pharma compounds which is detected in drinking water are very minimum magnitude than the minimum therapeutic dose.

The several organic solvents, colorants, acids, bases and a variety of other organic compounds are presented in pharmaceutical industry effluents, they are treated by aerobic process, photo-catalytic process and integrated process. The biogas generation, anaerobic decomposition of toxic effluents is attractive because of its low cost, which can complement energy requirements. There are a few reports on the photo-catalytic treatment of pharmaceutical effluent. The chloramphenicol (CAP) resistant bacteria or genes are found in water streams which are called as antibiotics and entering into the environment continuously [3]. The CAP is effective against both gram-positive and gram-negative bacteria. The CAP is expelled for use in food-producing animals in many countries such as USA, Canada, Australia, Japan, China and India [4]. The existence of traces of CAP showed around < 1 μgkg−1 by detection of veterinary drugs in manure, groundwater, soil and plants [5]. In China, CAP is detected as 26–2430 ngL^{-1} in influent and 3–1050 ngL^{-1} [6, 7] and 47.4 μgL^{-1} [8] in sewage treatment plant effluent.

The Advanced Oxidation Process (AOPs) [9-11], photo-catalysis process are the cost-effective method which is apply for the degradation of Chloramphenicol active compounds (CAC) [12] present in water. The TiO_2 is found to be capable of achieving complete oxidation of pollutants by generation of hydroxyl radicals ($HO^{\bullet}$) and valence band (vb) holes (h^+) created, when the catalyst is exposed to UV irradiation [12,13]. In this present work, we investigated the degradation behavior of CAP drug in the UV-TiO_2 [14, 15] photo-catalytic (UVPC) process using developed membrane materials for reduction in TOC. Hence, the main ideas are to (i) evaluate UVPC for the

*Address correspondence to this author at the Membrane Research Laboratory, Department of Chemical Engineering, National Institute of Technology, Tiruchirappalli–620 015,Tamil Nadu, India; Tel: +91 431 2503118; Fax: +91 431 2500133;
E-mail: arthanaree10@yahoo.com; arthanareeg@nitt.edu

E-ISSN: 2410-1869/23

decomposition of CAP molecule and its effectiveness for TOC reduction and (ii) identify the suitability of membranes for degradation products. This work also plan to study the removal of the antibiotic CAP using different types of oxidative processes.

2. MATERIALS AND METHODOLOGY

2.1. Materials

Titanium dioxide (TiO_2) powder (−325 mesh ≥99%) and Chloramphenicol ($Cl_2CHCONHCH(CH_2OH)CH(OH)C_6H_4NO_2$) were purchased from Sigma Aldrich, Hydrogen peroxide (H_2O_2) solution 30% w/v and Sulfuric acid (H_2SO_4) were purchased from Fisher Scientific, Hydrochloric acid (HCl) solution and Acetone (CH_3COCH_3) was purchased from Merck Life Science Pvt. Ltd., Polyether Sulfone (PES), Polyvinyl Alcohol (PVA), Cellulose tri-acetate (CTA), Cellulose Acetate (CA)[16], Dimethyl Formamide (DMF) $HCON(CH_3)_2$ and Glutaraldehyde ($C_5H_8O_2$) were purchased from LOBA Chemie.

2.1.1. Preparation of Chloramphenicol Stock Solution

Chloramphenicol stock solution was prepared by dissolving 500mg of CAP in 200 mL of distilled water (Figure **1**). To avoid contact with light, the beaker was covered with aluminium foil from all sides. The solution was stored at room temperature for further studies.

Figure 1: TiO_2 dissolved in water.

2.1.2. Sample Preparation

The pH of the distilled water was maintained at 5.5 with the help of 0.1M HCl for all studies. For sample preparation, 1mg of CAP in 100mL distilled water in a 250mL beaker. Beaker was covered with aluminium foil before adding any TiO_2 to prevent any degradation due to incident light (Figure **2**). Beaker was then kept on a magnetic stirrer at 400rpm for 10 minutes to break any clumps of TiO_2 present in the solution. Before loading the solution into a photocatalytic reaction 50µL of H_2O_2 was added to the solution. H_2O_2 acts as an oxidizing agent in an acidic medium and helps in increasing the photocatalytic efficiency. The same procedure was followed for different concentrations of Chloramphenicol and TiO_2.

Figure 2: TiO_2 and CAP solution on a magnetic stirrer at 400rpm.

2.1.3. Photocatalysis

The solution was then kept in the photo-catalytic reactor on a magnetic stirrer and was illuminated with a 40W UV lamp emitting UVA wavelengths between 300-400nm with a peak at 365nm. The solution was stirred at 400rpm to reduce the TiO_2 particles from settling at the bottom of the beaker. The reaction was carried out for 1 hour and 5 samples of 5mL each were taken at different time intervals (0min, 15min, 30min, 45min, 60min).

2.1.4. Heterogeneous TiO_2 Photo-Catalysis

The heterogeneous photo-catalysis (Figure **3**) employing the TiO_2 catalyst and widely utilized for reductive and oxidative reactions on its surface. When photon energy (He) greater than or equal to the bandgap energy of TiO_2 is illuminated onto its surface, usually 3.2eV (anatase) or 3.0 eV (rutile), the lone electron will be photoexcited to the empty conduction band in femtoseconds.

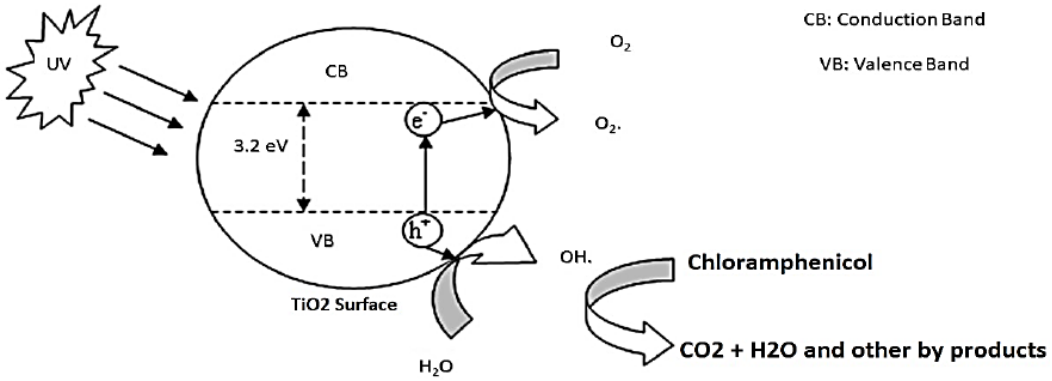

Figure 3: Mechanism of photo-catalytic reaction.

In heterogeneous photo-catalysis, the liquid phase organic compounds are degraded and water if the irradiation time is extended (Eq. (1)).

Organic Contaminants ⟶ Intermediate(s) ⟶ CO_2 + H_2O (1)

The overall photo-catalysis reaction can be explained as follows,

1. Mass transfer of the organic contaminants in the liquid phase on the TiO_2 surface.

2. Adsorption of the organic contaminants onto the photon-activated TiO_2 surface

3. Photo-catalysis reaction for the adsorbed phase on the TiO_2 surface.

4. Desorption of the intermediate(s) from the TiO_2 surface.

5. Mass transfer of the intermediate(s) from the interface region to the bulk fluid.

3. RESULTS AND DISCUSSION

3.1. Fourier Transform Infrared (FTIR) Spectroscopy of Membranes

The spectrum of the base PES membrane shows peaks at 1577 cm^{-1} and 1485 cm^{-1}, which are for aromatic bonds. The FTIR of PES membrane is appeared in Figure **4**. From the Figure **4**, The adsorption peaks at 1297 cm^{-1} and 1149 cm^{-1} are attributed to the asymmetric and symmetric stretching vibration of the sulfone (O=S=O) group. The sharp

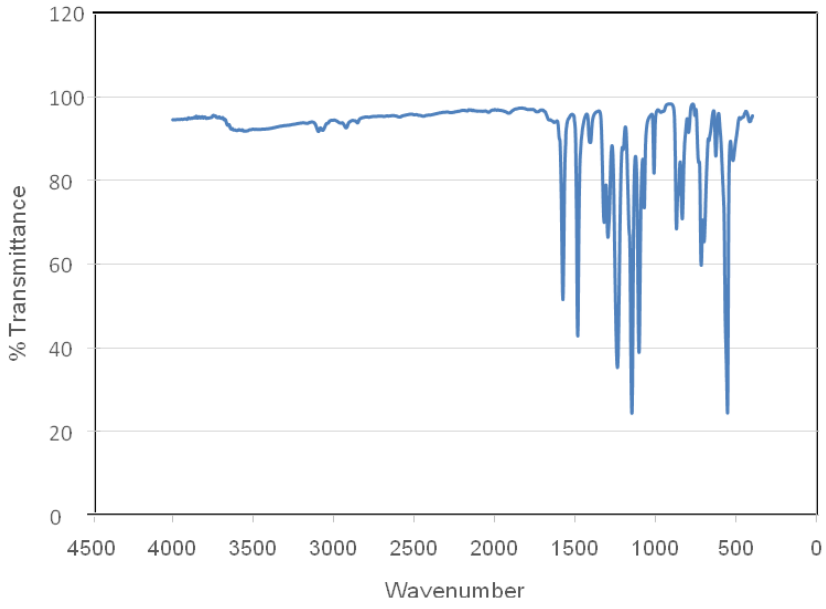

Figure 4: FTIR of PES membrane.

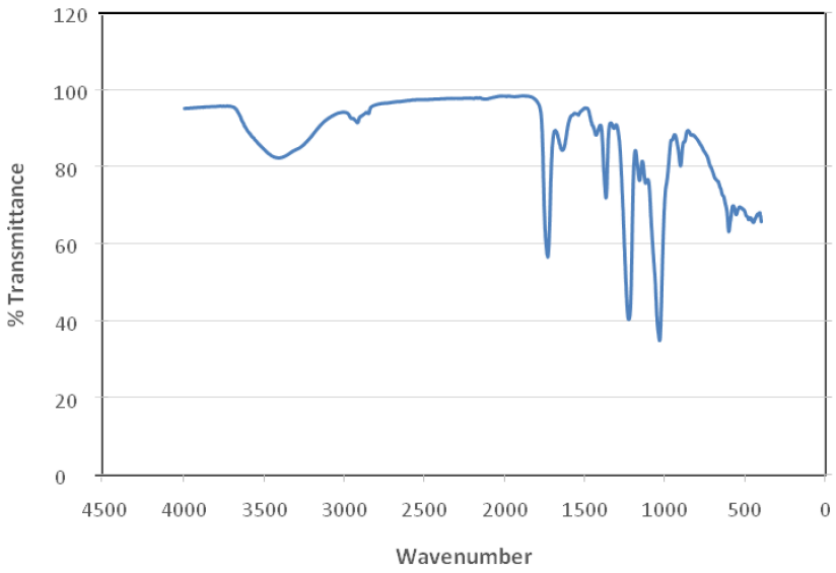

Figure 5: FTIR of CA membrane.

adsorption peak at 1239 cm^{-1} is due to the stretching vibration of the ether (Ar-O-Ar) linkage.

In the FTIR spectra, the CA membrane, the peak at 2870 and 2920 cm^{-1} appear on the membrane CA, which referred to the OH group [17].

Further, the range 1150-1050 cm−1 appeared the emergence of the C-O-C ether group in sharpening of the bands. For the CA membrane, the major adsorption features appeared at 1733 cm-1 (–C=O), 1370 cm-1 (–CH2), 1227 cm-1 (C–O), 1035 cm-1 (C– O–C) and 904 cm-1 (–CH).

As shown by the FI-IR spectra in Figure **6**, characteristic peaks were occurred at 1741 cm-1 for the C=O group and from 1035 cm^{-1} to 1210 cm^{-1} with the stretching vibration of C=O, C-CH_3, C-O-C, respectively. The acetyl groups of CTA might occurred during the membrane preparation [18].

3.2. Swelling and Contact Angle of the Membranes

From the Table **1** we can conclude that the PES-PVA membrane shows the most hydrophobicity followed by CTA-PVA and CA-PVA membranes from the contact angle and degree of swelling. In

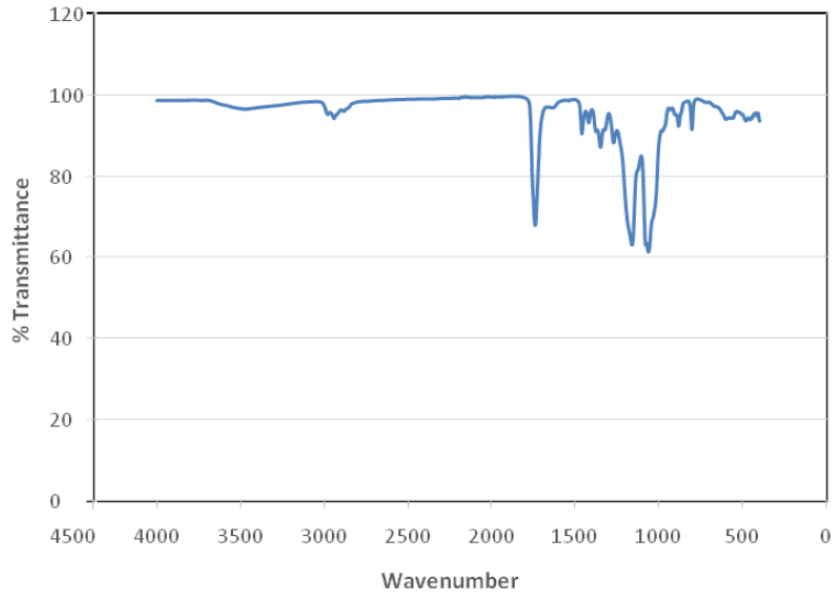

Figure 6: FTIR of CTA membrane.

hydrophilicity membrane is directly proportional to the contact angle and inversely proportional to the degree of swelling. The PES-PVA is having lower contact angle and more swelling degree when compared with other CA-PVA and CTA-PVA [19]. The may be due to the nature of polymer used in this work. The coating of PVA to the membrane casting solution favour the membrane porous and more hydrophilic. Hence, the all polymers altered the swelling and hydrophilic behaviours [20].

Table 1: Degree of Swelling and Contact Angle for Different Membranes

Membrane	Swelling Degree	Contact Angle (^{0})
PES-PVA	48.3±4.7	64.1±1.3
CTA-PVA	66.1±5.4	56.2±1.5
CA-PVA	72.5±6.5	51.8±1.4

3.3. Morphology of the Membranes

The SEM images of top layer PES and PES-PVA membranes were taken in Figure **7**. PES membrane facilitated a rapid phase resulting in micro void formation. It is observed that in PES in the presence of PVA, the membrane morphologies changed gradually. After coating of PVA tends to increase the number of membrane pores has been proven and the size of the macro voids was increased.

The two distinct layers can be observed in PES and PES-PVA membranes, a thin dense layer on the top and a typical sponge structure sub-layer on the bottom [21]. It is observed that the 100 wt.% CTA membrane, which facilitated a rapid phase and resulted in macro void formation. It is observed that in CTA in the presence of PVA, the membrane morphologies changed gradually. After adding PVA tends to increase the number of membrane pores has been proven and the size of the macro voids was decreased. The two distinct layers can be observed in CTA and CTA-PVA membranes (Figure **8**), a thin dense layer on the top and typical sponge structure sub layer on the bottom [22].

SEM top layer images of CA and CA-PVA membranes in Figure **9**. In the top layer a rapid phase that resulted in microvoid formation in 100% CA membrane. It is observed that in CA in the presence of PVA, the membrane morphologies changed gradually. As a result, the size of the macro voids was increased. The number of membrane pores has been increased in CA-PVA membrane and obviously shown by the membranes surface structure. The two layers can be observed in CA and CA-PVA (Figure **9**) membranes, a thin dense layer on the top and typical sponge structure sub layer on the bottom [23]. The coating can be clearly seen on the surface of the membrane alone with the pores of the membrane.

3.4. Ultra Violet (UV) Analysis

3.4.1. UV analysis of Chloramphenicol

Figure **10** represents the UV spectrum analysis of Chlorampehnicol Absorbance and the wavelength. UV spectrum of Chloramphenicol was obtained by loading 25mg/L concentration of Chloramphenicol. The different intervals of Absorbance Chloramphenicol wavelength range was selected between 200-350nm

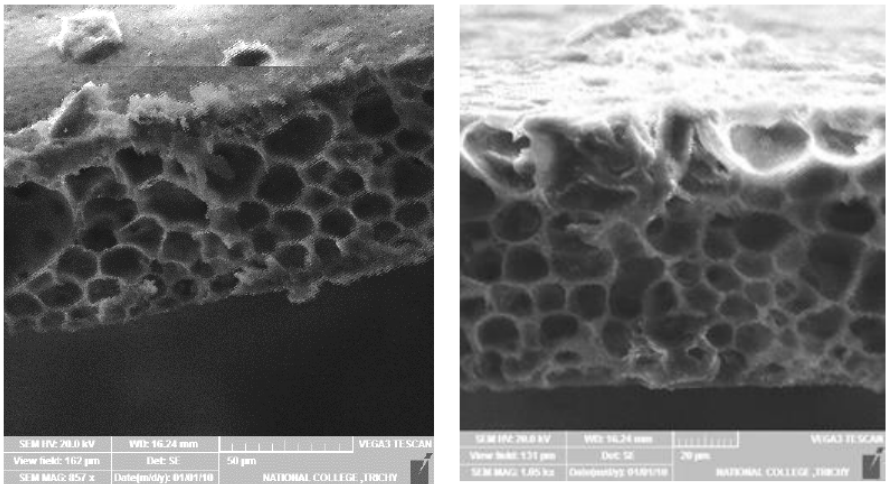

PES membrane **PES-PVA membrane**

Figure 7: SEM analysis of PES membrane with and without PVA coating.

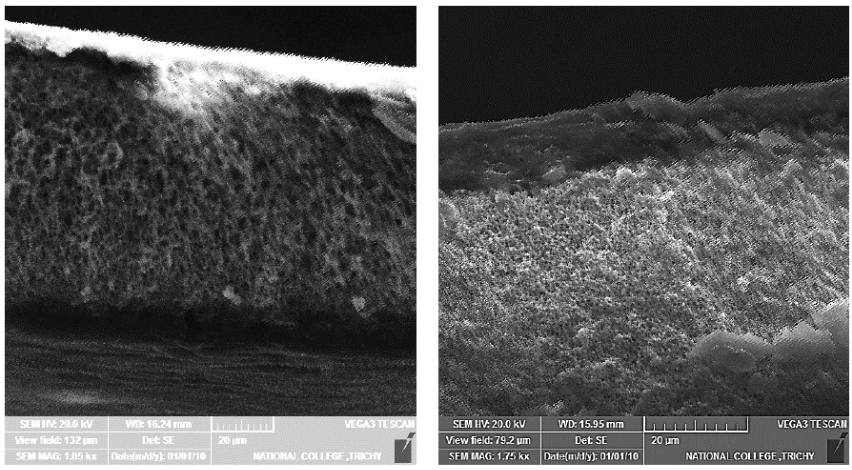

Figure 8: SEM analysis of CTA membrane with and without PVA coating.

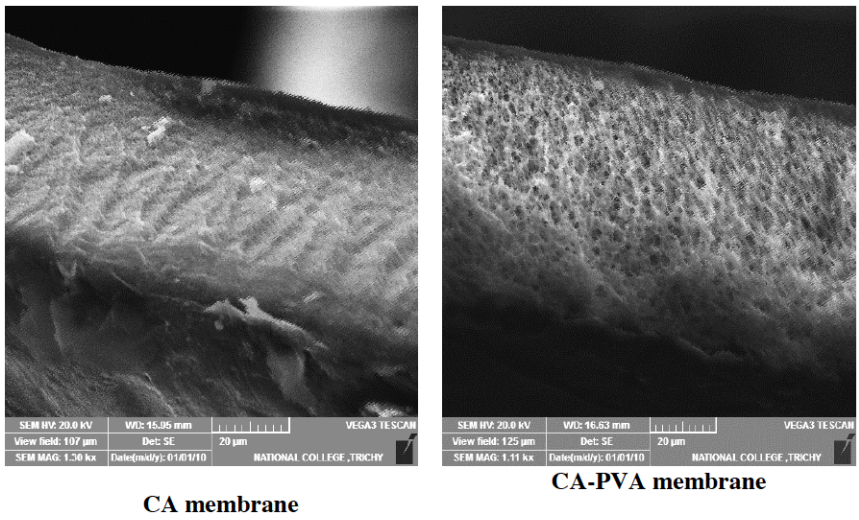

Figure 9: SEM analysis of CA membrane with and without PVA coating.

[24]. Maximum peak was obtained at 277nm which was further taken to determine the absorbance.

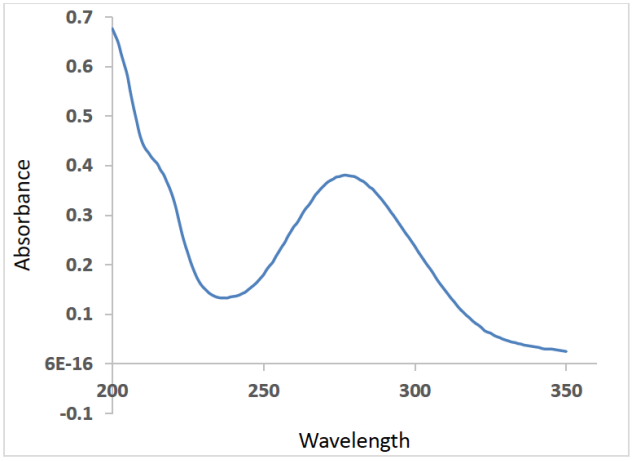

Figure 10: UV Spectrum of Chloramphenicol.

3.4.2. Kinetic study with TiO_2 concentration of 0.5gm/L

Figure **11** represents the percentage degradation of CAP with TiO_2 under UV at different time intervals.As time increases the degradation increases and approaches linearity. It was observed that the percentage degradation occurs maximum with 10mg/L CAP and minimum with 30mg/L CAP. As a control, a solution of TiO_2 and CAP was kept in dark for 1 hour and measured. A solution of CAP and TiO_2 at the dark stage, percentage degradation zero level at different time intervals. In the Table **2**, $-\ln C/C_0$ was calculated for different concentration of CAP at 0.5gm/L of TiO_2 to calculate the kinetics of the reaction.

Figure **12** represents the percentage degradation of CAP with TiO_2 under UV at different time intervals. The Different concentration of CAP (10mg/L, 20mg/L, and

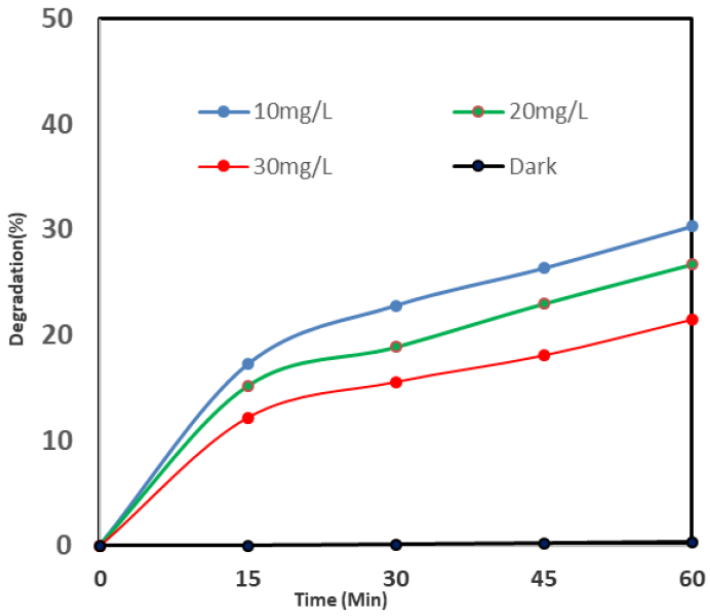

Figure 11: Percentage degradation of different concentration CAP at 0.5gm/L TiO_2.

30mg/L) and 0.5gm/L TiO_2 we chosen and photocatalytically degraded. As the time increases the degradation increases and approached towards linearity [25].

Table 2: -lnC/C_0 at Different Concentration of CAP and Different Time Intervals at 0.5gm/L TiO_2

Time (min)/Conc. (mg/L)	10mg/L	20mg/L	30mg/L
0min	0	0	0
15min	0.1888	0.1644	0.1298
30min	0.2588	0.2089	0.1689

3.4.2. Kinetic Study with TiO_2 Concentration of 0.5gm/L

It was observed that the percentage degradation occurs maximum with 10mg/L CAP and minimum at 30mg/L CAP. As a control, a solution of TiO_2 and CAP was kept under dark for 1 hour and measured. A solution of CAP and TiO_2 at Dark stage, percentage degradation zero level at different time intervals.

The rate of reaction of CAP at 0.5gm/L TiO_2 at different time intervals in Figure **12**. The rate of reaction and reaction constant was found by plotting the line and finding the equation of the line. Only the first 30

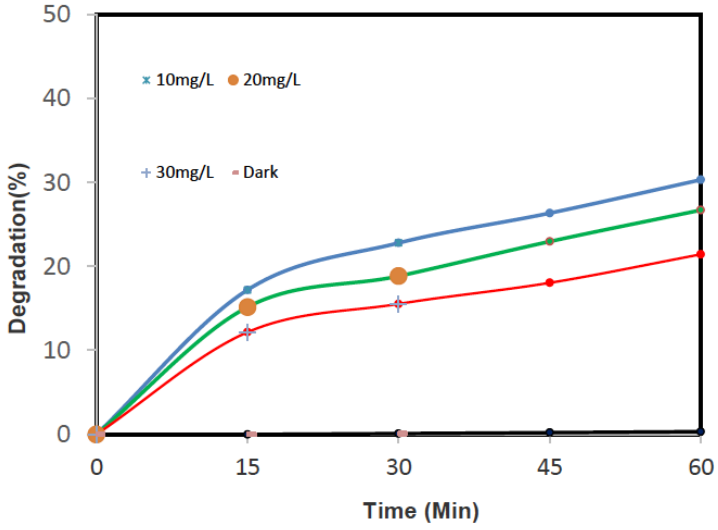

Figure 12: Time vs - lnC/C_0 plot of CAP at 0.5gm/L TiO_2.

Table 3: Calculation of Various Kinetic Factors at 0.5gm/L of TiO_2

Kinetic factors	Unit	Concentration (mg/L)		
		10	20	30
r	(mg L^{-1} min^{-1})	0.094	0.156	0.186
k	(min^{-1})	0.0094	0.0078	0.0062
$1/C_0$	(mg L^{-1})	0.1	0.05	0.333
1/r	(mg^{-1} L min)	10.63	6.41	5.37
R^2	--	0.9212	0.8813	0.8948

minutes of the reaction is taken as to reduce the interference of the intermediate products on the reaction kinetics. The rate of reaction and rate constant was shown in Table **3**. The rate of reaction is increased with the increase in the CAP concentration showing rate of reaction of 30 mg/L of CAP as a maximum [26].

Figure **13** represents the percentage degradation of CAP at the different time intervals of TiO_2 in 1mg/L under UV. In this study, at different concentrations of CAP of 10mg/L,20mg/L and 30 mg/L and the concentration of TiO_2 was kept in 1mg/L and degraded by photo catalytically.

The percentage degradation value is maximum occurred in 10mg/L and minimum value is occurred in 30 mg/L CAP at 1mg/L TiO2. But dark control percentage degradation value is zero at different time interval. In Table **4**, $-\ln C/C_0$ was calculated for different concentration of CAP at 1gm/L of TiO_2 to calculate the kinetics of the reaction.

Table 4: Time vs $-\ln C/C_0$ at Different Concentration of CAP and Different Time Intervals at 1gm/L TiO_2

Time (min)	Concentration (mg/L)		
	10	20	30
15	0.2265	0.1867	0.1663
30	0.3176	0.2554	0.2305

Figure **14** represents the rate of reaction is measured of CAP at 1 mg/L of TiO_2 for 30-minute time intervals. The rate of reaction was found by plotting the line and finding the equation of the line. The rate of reaction gradually increases from zero-time intervals to 30 minutes of CAP at 1 mg/L of TiO_2. The reaction rate is taken in only the first 30 minutes to reduce the

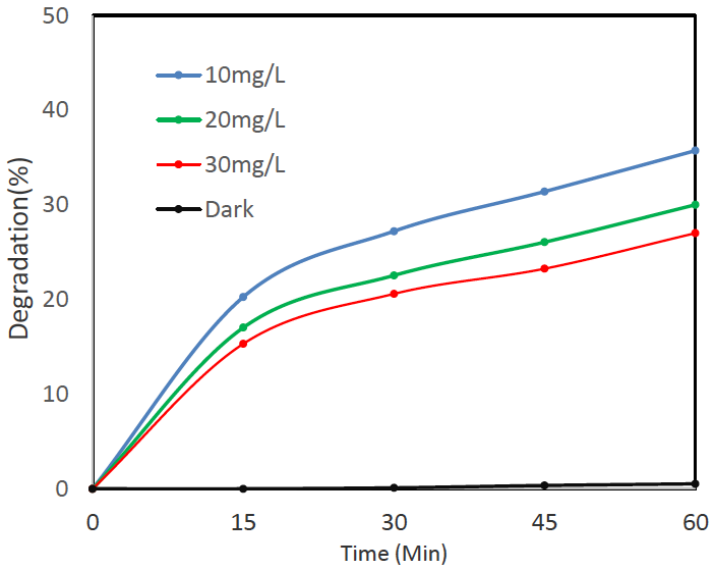

Figure 13: Percentage degradation of different concentration CAP at 1gm/L TiO_2.

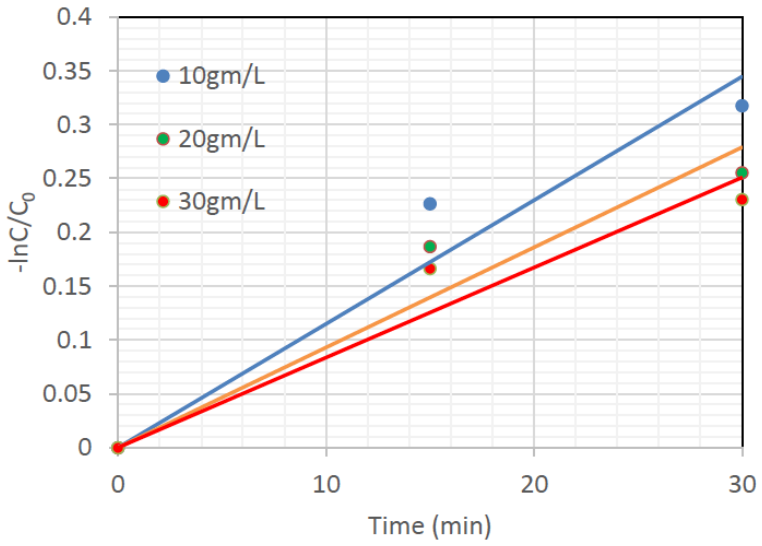

Figure 14: Time vs -lnC/C_0 plot of CAP at 1gm/L TiO_2.

interference of the intermediate products on the reaction kinetics. The rate of reaction and rate constant were shown in Table **4.4**. The rate of reaction is increased with the increase in the CAP concentration from 10 mg/L to 30 mg/L, it showing the rate of reaction as a maximum of 30mg/L.

The rate of reaction and rate constant was shown in Table **5**. The rate of reaction is increased with the increase in the CAP concentration showing rate of reaction of 30mg/L of CAP as a maximum [27]. Figure **15** represents the percentage degradation of CAP under UV at different time intervals. In this study, some concentrations of CAP were chosen (10mg/L, 20mg/L and 30mg/L) and the concentration of TiO_2 was kept at 1.5gm/L and photo catalytically degraded. The maximum value of percentage degradation occurred in 10 mg/L CAP for 60 minutes at 1.5 gm/L TiO_2 and the minimum value of percentage degradation occurred in 30 mg/L for 60 minutes at 1.5 gm/L TiO_2.

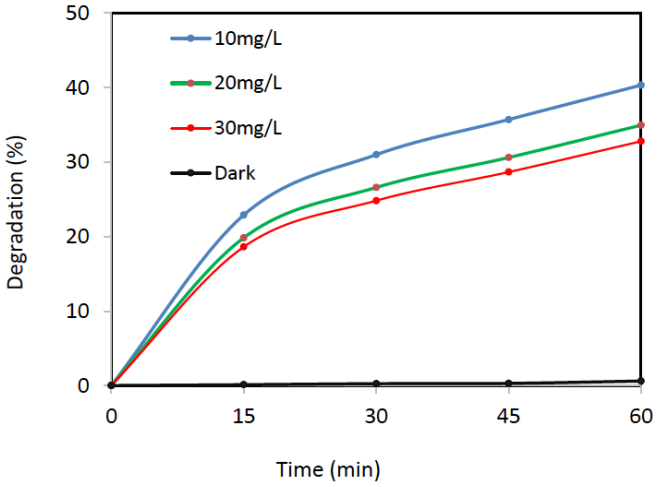

Figure 15: Percentage degradation of different concentration CAP at 1.5gm/L TiO_2.

3.4.4. Kinetic Study with TiO_2 Concentration of 1.5gm/L

In this study, time increases the degradation value is increased and approached towards linearity. As a

Table 5: Calculation of Various Kinetic Factors at 1gm/L of TiO_2

Kinetic factors	Unit	Concentration (mg/L)		
		10	20	30
r	(mg L^{-1} min^{-1})	0.115	0.186	0.252
k	(min^{-1})	0.0115	0.0093	0.0084
$1/C_0$	(mg L^{-1})	0.1	0.05	0.333
1/r	(mg^{-1} L min)	8.69	5.37	3.96
R^2	--	0.9315	0.9203	0.9263

dark control, a solution of TiO_2 and CAP was measured. In this study, the percentage degradation value is zero at different time intervals.

In Table **6**., $-\ln C/C_0$ was calculated for different concentration of CAP at 1.5gm/L of TiO_2 to calculate the kinetics of the reaction. The rate of reaction is measured in different concentrations of CAP (10 mg/L, 20 mg/ L and 30 mg/L) at different time intervals in Figure **16**. The rate of reaction is increased in 10 mg/L of CAP at 1.5 gm/L of Tio_2. The rate of reaction and reaction constant was found by plotting the line and finding the equation of the line.

Table 6: $\ln C/C_0$ at Different Concentration of CAP and Different Time Intervals at 1.5gm/L TiO_2

Time (min)	Concentration (mg/L)		
	10	20	30
15	0.2599	0.221	0.206
30	0.3709	0.3091	0.2852

The rate of reaction is taken as reducing the interference of the intermediate products on the reaction kinetics in the first 30 minutes [28]. The maximum value of the rate of reaction is measured in 10mg/L of CAP at 1.5gm/L of TiO_2 in 30 minutes and the minimum value is measured in 30mg/L of CAP at 1.5gm/L of Tio_2 in 30 minutes. The rate of reaction and rate of constant were measured in different concentrations of CAP at 1.5 gm/L of TiO_2.

The rate of reaction and rate constant was shown in Table **7**. The rate of reaction is increased with the increase in the CAP concentration showing rate of reaction of 30mg/L of CAP as a maximum.

3.4.5. Kinetic Study with TiO_2 Concentration of 2gm/L

Figure **17** represents the percentage degradation of CAP under UV at different time intervals. In this study, some concentrations of CAP were chosen (10mg/L, 20mg/L and 30mg/L) and the concentration of TiO_2 was kept at 2gm/L and photo catalytically degraded. The

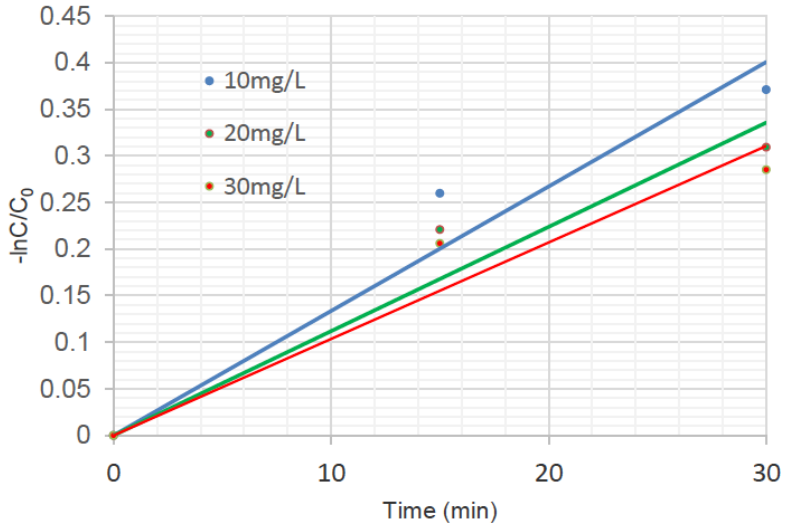

Figure 16: Time vs $-\ln C/C_0$ plot of CAP at 1.5gm/L TiO_2.

Table 7: Calculation of Various Kinetic Factors at 1.5gm/L of TiO_2

Kinetic Factors	Unit	Concentration (mg/L)		
		10	20	30
r	(mg L^{-1} min^{-1})	0.134	0.224	0.312
k	(min^{-1})	0.0134	0.0112	0.0104
$1/C_0$	(mg L^{-1})	0.1	0.05	0.333
1/r	(mg^{-1} L min)	7.46	4.46	3.20
R^2	--	0.9388	0.9303	0.9258

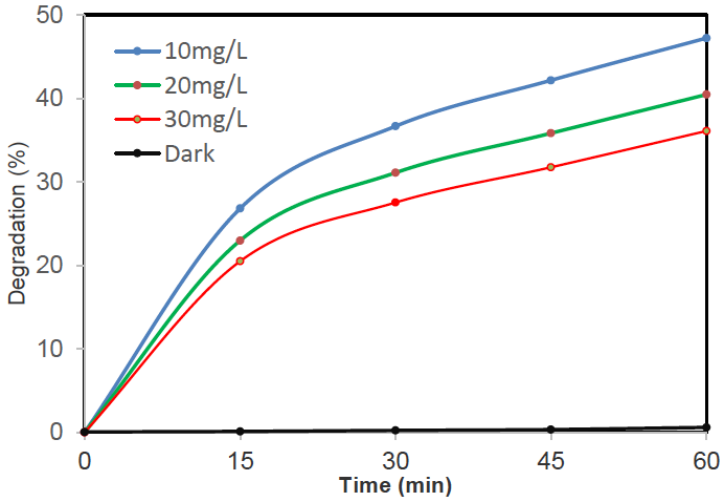

Figure 17: Percentage degradation of different concentration CAP at 2gm/L TiO_2.

maximum value of percentage degradation occurred in 10mg/L CAP for 60 minutes at 2gm/L TiO_2 and the minimum value of percentage degradation occurred in 30mg/L for 60 minutes at 2gm/L TiO_2. In this study, time increases the degradation value is increased and approached towards linearity. As a dark control, a solution of TiO_2 and CAP was measured. In this study, the percentage degradation value is zero at different time intervals.

This experiment was performed with the same CAP concentration at 2gm/L of TiO_2 for 1 hour and the degradation was observed at a different time interval. As a control, a solution of TiO_2 and CAP was kept in dark for 1 hour and measured. The percentage degradation value is zero in a solution of CAP and TiO_2 at dark control.

In Table **8**, the rate of reaction is decreased from 10 mg/L of CAP at 2gm/L of TiO_2 to 30 mg/L of CAP at 2gm/L of TiO_2 at different time intervals. $-\ln C/C_0$ was calculated for different concentrations of CAP at 2gm/L of TiO_2 to calculate the kinetics of the reaction.

Table 8: $-\ln C/C_0$ at Different Concentration of CAP and Different Time Intervals at 2gm/L TiO_2

Time (min))	Concentration (mg/L)		
	10	20	30
15	0.3119	0.2608	0.2292
30	0.4566	0.3724	0.3219

Figure **18** represents the rate of reaction is measured in different concentrations of CAP (10 mg/L,

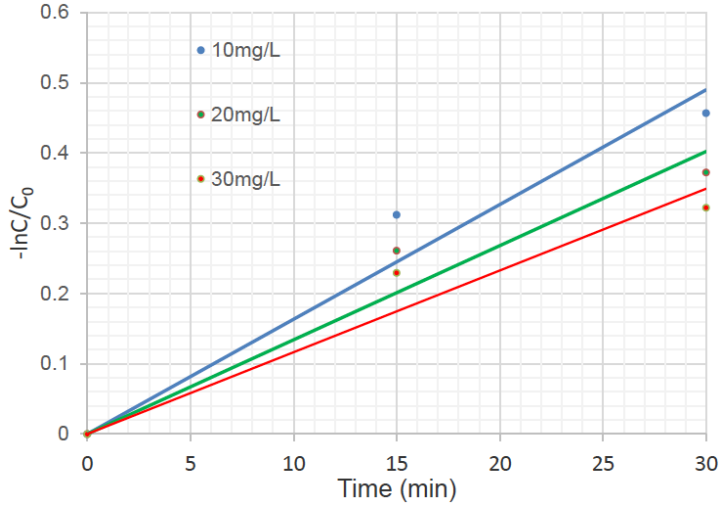

Figure 18: Time vs $-\ln C/C_0$ plot of CAP at 2gm/L TiO_2.

Table 9: Calculation of Various Kinetic Factors at 1.5gm/L of TiO_2

Kinetic Factors	Unit	Concentration (mg/L)		
		10	20	30
r	(mg L^{-1} min^{-1})	0.163	0.268	0.348
k	(min^{-1})	0.0163	0.0134	0.0116
$1/C_0$	(mg L^{-1})	0.1	0.05	0.333
1/r	(mg^{-1} L min)	6.13	3.73	2.87
R^2	--	0.9487	0.9391	0.9321

20 mg/ L and 30 mg/L) at different time intervals. The rate of reaction is increased in 10 mg/L of CAP at 2gm/L of Tio_2. The rate of reaction and reaction constant was found by plotting the line and finding the equation of line. The rate of reaction is taken as reduce the interference of the intermediate products on the reaction kinetics in the first 30 minutes. The maximum value of the rate of reaction is measured in 10 mg/L of CAP at 2gm/L of TiO_2 in 30 minutes and the minimum value is measured in 30 mg/L of CAP at 2gm/L of TiO_2 in 30 minutes. The rate of reaction and rate of constant were measured in different concentrations of CAP at 2 gm/L of TiO_2.

The rate of reaction and rate constant was shown in Table **9**. The rate of reaction is increased with the increase in the CAP concentration showing rate of reaction of 30mg/L of CAP as a maximum. The rate of reaction at different catalyst concentrations (0.5gm/L, 1gm/L, 1.5gm/L and 2gm/L) was observed from the previous experiments and plotted in a $1/r_0$ vs $1/C_0$ graph as shown in Figure **19**.

3.4.6. Rate of Adsorption at Different Catalyst Concentrations

A straight line was observed from which the slope and intercept were calculated from which the adsorption constant was finally calculated. Slope, intercept and adsorption constant are the maximum value find out at different catalyst concentrations. In Table **10**, the adsorption kinetics are calculated.

4. LC-MS OF PHOTO-CATALYTICALLY DEGRADED POLLUTANT

In order to find the degraded products, which will further be separated by pervaporation, LC-MS of the solution was done after 1 hour of degrading the solution photo catalytically. In order to avoid further degradation sample was collected and wrapped in foil

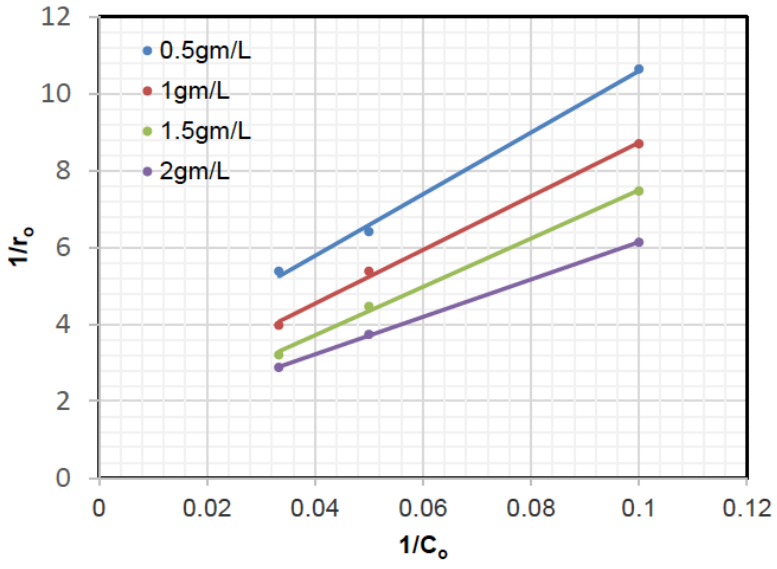

Figure 19: $1/r_0$ vs $1/C_o$ plot at different catalyst concentration.

Table 10: Calculation of Parameters of Adsorption Kinetics

Concentration (gm/L))	Adsorption kinetics		
	$1/k_rK$	$1/k_r$(mg^{-1} L min)	K(mg^{-1} L)
0.5	80.196	2.575	0.032
1	69.841	1.7461	0.025
1.5	62.941	1.1983	0.019

until LC-MS was performed. The spectrum of LC-MS with different *m/z* ratios is shown in Figure **20**. From the results obtained, it can be concluded that most of the compounds which were formed as intermediated were aromatic compounds.

CONCLUSIONS

The effective technique of AOP has been proven to be in degradation of the organic compound under the effect of UV radiation. From the experimental study UV spectra of chloramphenicol shoes the maximum absorbance at 277nm. The maximum percentage of degradation occurs at 10mg/L of CAP and 2gm/L of TiO_2. As the concentration of CAP increased, the percentage degradation decreased. Also, the concentration of catalyst increased, the percentage of degradation is increased. With the increase in the concentration of CAP, the reaction rate is found to be decreasing and the rate of reaction is found to be increasing. From the plot of $1/r_0$ vs $1/C_0$, it was found that the adsorption rate constant decreases up to

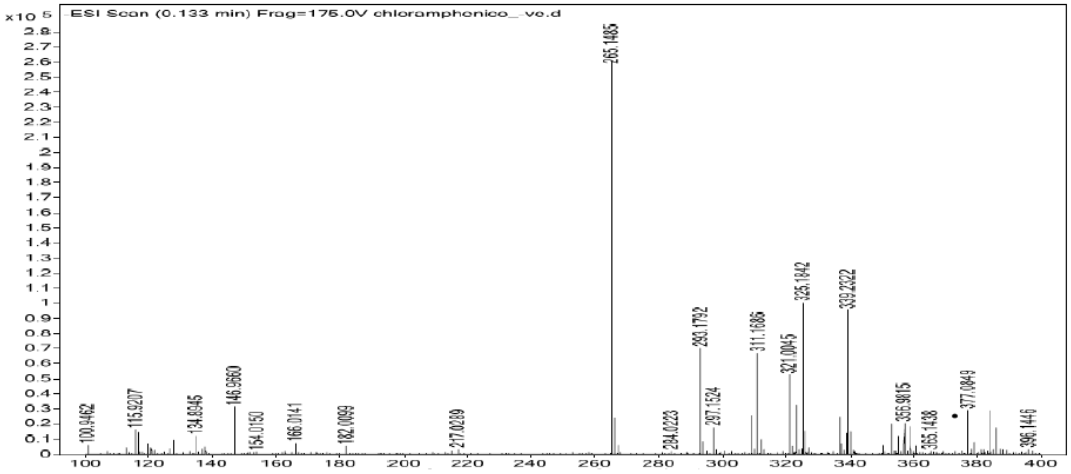

Figure 20: Mass Spectrum of photocatalytically degraded CAP.

Table 11: Degraded Products of CAP Obtained from Photocatalysis

Compound Name	m/z	t_r (mins)	Mass
Chloramphenicol	321.0044	9.06	322.0116
Pyroglutamic acid (used in various skin and hair products)	128.0354	8.52	129.0427
Chlorthalidone (use to treat high blood pressure)	336.9989	9.06	338.0061
Quinolinic acid (intermediate to produce pharmaceuticals and metal salts)	166.0142	9.42	167.0216
4-Hydrobenzoic Acid (used in the manufacturing of various drugs)	134.8945	9.78	135.9018
M*et a*la Met	350.124	11.04	351.1317
5-(4-hydroxy-2,5-dimethylphenoxy)-2,2-dimethyl-Pentanoic acid (Gemfibrozil M1)	265.1484	9.18	266.1554

1.5gm/L of TiO_2 and increases at 2gm/L of TiO_2. Analysis of degraded solution with LC-MS revealed the intermediate products which were analyzed as aromatic and volatile organic compounds. Among membranes, the PES-PVA membrane shows the most hydrophobicity followed by CTA-PVA and CA-PVA. FTIR analysis of membranes showed the different organic bonds in the membranes and concluded that membranes were cast well. From the SEM images, we can conclude that PVA coating on the membrane was done well.

REFERENCES

[1] Allen J, Cole S, Hand K, Herbert S, Hinton J, Ismail N, *et al*. J Infect. 2011; 63(6): e56-7. https://doi.org/10.1016/j.jinf.2011.04.104

[2] Bacchus AN, Javor GT. Stability of Escherichia coli membrane proteins during chloramphenicol treatment. AntimicrobAgents Chemother. 1975; 8(3): 387-9. https://doi.org/10.1128/AAC.8.3.387

[3] Parsley LC, Consuegra EJ, Kakirde KS, Land AM, Harper WF, Liles MR. Appl Environ Microbiol. 2010; 76(11): 3753-7. https://doi.org/10.1128/AEM.03080-09

[4] Amrish Tyagi, Srinivas Das, and K K Singhal, Indian Journal of Animal Sciences, 2008; 78(5): 510-514

[5] Hu Q, Milenkovic L, Jin H, Scott MP, Nachury M V., Science (80-). 2010; 329(5990): 436-9. https://doi.org/10.1126/science.1191054

[6] Lin H, Hopmans JW, Richter D deB. Vadose Zo J. 2011; 10(3): 781-5. https://doi.org/10.2136/vzj2011.0084

[7] Xu A, Haines N, Dlugosz M, Rana NA, Takeuchi H, Haltiwanger RS, *et al*. In vitro reconstitution of the modulation of Drosophila Notch-ligand binding by fringe. J Biol Chem. 2007; 282(48): 35153-62. https://doi.org/10.1074/jbc.M707040200

[8] Liu P, Zhang H, Feng Y, Yang F, Zhang J. Chem Eng J. 2014; 240: 211-20. https://doi.org/10.1016/j.cej.2013.11.057

[9] Hapeshi E, Achilleos A, Papaioannou A, Valanidou L, Xekoukoulotakis NP, Mantzavinos D, *et al*. Water Sci Technol. 2010; 61(12): 3141-6. https://doi.org/10.2166/wst.2010.921

[10] Akbari MZ, Xu Y, Lu Z, Peng L. Review of antibiotics treatment by advance oxidation processes. Environ Adv. 2021; 5: 100111. https://doi.org/10.1016/j.envadv.2021.100111

[11] Elmolla ES, Chaudhuri M. Desalination. 2010; 256(1-3): 43-7. https://doi.org/10.1016/j.desal.2010.02.019

[12] Petala M, Tsiridis V, Samaras P, Zouboulis A, Sakellaropoulos GP. Desalination. 2006; 195(1-3): 109-18. https://doi.org/10.1016/j.desal.2005.10.037

[13] Akira Fujishima Xintong Zhangb, Donald A. Tryk, Surface Science Reports 63,12 515-582 (2008) https://doi.org/10.1016/j.surfrep.2008.10.001

[14] Hu CW, Li M, Cui YB, Li DS, Chen J, Yang LY. Toxicological effects of TiO2 and ZnO nanoparticles in soil on earthworm Eisenia fetida. Soil Biol Biochem. 2010; 42(4): 586-91. https://doi.org/10.1016/j.soilbio.2009.12.007

[15] Ren J, Song H, Guo H, Yao Z, Wei Q, Jiao K, *et al*. J Clean Prod. 2021; 325(October): 129332. https://doi.org/10.1016/j.jclepro.2021.129332

[16] Sivakumar M, Mohan D, Rangarajan R.. Polym Int. 1998; 47(3): 311-6. https://doi.org/10.1002/(SICI)1097-0126(199811)47:3<311::AID-PI51>3.0.CO;2-2

[17] Ali M, Zafar M, Jamil T, Butt MT. Desalination. 2011; 1; 270(1-3): 98-104. https://doi.org/10.1016/j.desal.2010.11.027

[18] Ebrahim S, Morsy A, Kenawy E, Abdel-Fattah T, Kandil S. Desalination and Water Treatment. 2016; 57(44): 20738-48.

[19] Olivares Moreno CA, Altintas Z. Membranes. 2022; 12(11): 1117. https://doi.org/10.3390/membranes12111117

[20] Chen L, Li F, Jiang L, He F, Wei Y. J. Water Process Eng. 2022; 48: 102887. https://doi.org/10.1016/j.jwpe.2022.102887

[21] Chang CC, Yu ST, Su JF, Cheng LP. J. Polym. Res. 2022; 29: 1-0. https://doi.org/10.1007/s10965-021-02867-6

[22] Noorjahan SE, Sekar S, Sastry TP. Current Science. 2008; 10: 958-62.

[23] Han J, Lee W, Choi JM, Patel R, Min BR. J Membr. Sci. 2010; 351(1-2): 141-8. https://doi.org/10.1016/j.memsci.2010.01.038

[24] Khudzaifah NA, Basukiwardojo MM. World J Advan. Rese. and Revi. 2022; 15(1): 525-33. https://doi.org/10.30574/wjarr.2022.15.1.0719

[25] Zhang J, Zhao R, Cao L, Lei Y, Liu J, Feng J, Fu W, Li X, Li B. J Hazar. Mater. 2020; 384: 121344. https://doi.org/10.1016/j.jhazmat.2019.121344

[26] Cao Y, Qiu W, Zhao Y, Li J, Jiang J, Yang Y, Pang SY, Liu G. Chemi. Eng. J. 2020; 401: 126146. https://doi.org/10.1016/j.cej.2020.126146

[27] Wu X, Zhuang X, Lv Z, Xin F, Dong W, Li Y, Jia H. Envir. Sci. Water Rese. & Techno. 2022; 8(11): 2531-44. https://doi.org/10.1039/D2EW00363E

[28] Dong H, Fu Y, Wang P, Jiang W, Gao G, Zhang X. Environ. Pollu. 2022; 301: 119031. https://doi.org/10.1016/j.envpol.2022.119031

Received on 21-12-2022 Accepted on 08-02-2023 Published on 07-03-2023

DOI: https://doi.org/10.15379/2410-1869.2023.10.01.03